OXFORD

Cerebral Cortex, 2022, **32**, 3042–3056
https://doi.org/10.1093/cercor/bhab399
Advance access publication date: 18 November 2021
Original Article

Abnormal whisker-dependent behaviors and altered cortico-hippocampal connectivity in *Shank3b*$^{-/-}$ mice

Luigi Balasco[1], Marco Pagani[2], Luca Pangrazzi[1], Gabriele Chelini[1], Alessandra Georgette Ciancone Chama[1], Evgenia Shlosman[1], Lorenzo Mattioni[3], Alberto Galbusera[2], Giuliano Iurilli[4], Giovanni Provenzano[3], Alessandro Gozzi[2], Yuri Bozzi[1,5,*]

[1]CIMeC - Center for Mind/Brain Sciences, University of Trento, 38068 Rovereto, TN, Italy,
[2]Functional Neuroimaging Laboratory, Center for Neuroscience and Cognitive Systems, Istituto Italiano di Tecnologia, 38068 Rovereto, TN, Italy,
[3]Department of Cellular, Computational, and Integrative Biology (CIBIO), University of Trento, 38123 Trento, Italy,
[4]Systems Neurobiology Laboratory, Center for Neuroscience and Cognitive Systems, Istituto Italiano di Tecnologia, 38068 Rovereto, TN, Italy,
[5]CNR Neuroscience Institute, 56124 Pisa, Italy

*Corresponding author: Yuri Bozzi, Center for Mind/Brain Sciences (CIMeC) - University of Trento, Piazza della Manifattura 1, 38068 Rovereto (TN), Italy. Email: yuri.bozzi@unitn.it

Abnormal tactile response is an integral feature of Autism Spectrum Disorders (ASDs), and hypo-responsiveness to tactile stimuli is often associated with the severity of ASDs core symptoms. Patients with Phelan-McDermid syndrome (PMS), caused by mutations in the SHANK3 gene, show ASD-like symptoms associated with aberrant tactile responses. The neural underpinnings of these abnormalities are still poorly understood. Here we investigated, in *Shank3b*$^{-/-}$ adult mice, the neural substrates of whisker-guided behaviors, a key component of rodents' interaction with the surrounding environment. We assessed whisker-dependent behaviors in *Shank3b*$^{-/-}$ adult mice and age-matched controls, using the textured novel object recognition (tNORT) and whisker nuisance (WN) test. *Shank3b*$^{-/-}$ mice showed deficits in whisker-dependent texture discrimination in tNORT and behavioral hypo-responsiveness to repetitive whisker stimulation in WN. Sensory hypo-responsiveness was accompanied by a significantly reduced activation of the primary somatosensory cortex (S1) and hippocampus, as measured by c-*fos* mRNA induction, a proxy of neuronal activity following whisker stimulation. Moreover, resting-state fMRI showed a significantly reduced S1-hippocampal connectivity in *Shank3b* mutants, in the absence of altered connectivity between S1 and other somatosensory areas. Impaired crosstalk between hippocampus and S1 might underlie *Shank3b*$^{-/-}$ hypo-reactivity to whisker-dependent cues, highlighting a potentially generalizable somatosensory dysfunction in ASD.

Key words: autism; connectivity; hippocampus; mouse; somatosensory.

Introduction

Autism spectrum disorders (ASDs) represent a heterogeneous group of neurodevelopmental disorders characterized by social interactions and communication deficits, accompanied by restricted and stereotyped behaviors (American Psychiatric Association 2013). Several studies also indicate that abnormal sensory processing is a crucial feature of ASD. About 90% of ASD individuals have atypical responses to different types of sensory stimuli (Robertson and Baron-Cohen 2017), and sensory abnormalities (described as both hyper- or hypo-reactivity to sensory stimulation) are currently recognized as diagnostic criteria of ASD (American Psychiatric Association 2013). Several pieces of evidence support the idea that altered sensory perception underlies ASD patients' ability to interact with the surrounding environment, especially in the presence of novel stimuli and unexpected context (Robertson and Baron-Cohen 2017). Both over- and under-responsiveness to tactile stimuli are frequently observed in ASD and fall under the general term of tactile defensiveness (Mikkelsen et al. 2018; Balasco et al. 2020). Most importantly, abnormal responses to tactile stimuli correlate with and predict the severity of ASD. Hypo-responsiveness to tactile stimuli is associated with higher severity of ASD core symptoms (Foss-Feig et al. 2012), and touch avoidance during infancy is predictive of ASD diagnosis in toddlers (Mammen et al. 2015).

Phelan-McDermid syndrome (PMS) is a neurodevelopmental disorder characterized by ASD-like behaviors, developmental delay, intellectual disability, and absent or severely delayed speech (Phelan and McDermid 2012). PMS is caused by mutations in the SHANK3 gene coding for SH3 and multiple ankyrin repeat domains protein 3 (Leblond et al. 2014; Monteiro and Feng 2017), a crucial component of excitatory postsynaptic density (Naisbitt et al. 1999; Jiang and Ehlers 2013). Patients with

Received: March 24, 2021. **Revised:** October 6, 2021. **Accepted:** October 7, 2021

PMS often show somatosensory processing dysfunction, including over-sensitiveness to touch and tactile defensiveness (Philippe et al. 2008).

Altered somatosensory responses have been recently described in mouse strains harboring mutations in ASD-relevant genes, suggesting that whisker-dependent behaviors are a good proxy to study somatosensory processing defects relevant for ASD (Balasco et al. 2020; Orefice 2020). Mice use their whiskers to explore objects (Brecht 2007) and interact with conspecifics (Ahl 1986), thus allowing a detailed representation of the surrounding environment during navigation (Petersen 2007; Diamond et al. 2008).

Mice lacking the *Shank3* gene are widely considered as a reliable model to study ASD-like symptoms relevant to PMS (Peça et al. 2011; Jaramillo et al. 2017). Interestingly, *Shank3b*$^{-/-}$ mutant mice display aberrant whisker-independent texture discrimination and over-reactivity to tactile stimuli applied to hairy skin (Orefice et al. 2016). More recent findings showed that developmental loss of *Shank3* in peripheral somatosensory neurons (that causes over-reactivity to tactile stimuli) also results in ASD-like behaviors in adulthood (Orefice et al. 2019). While deficits of peripheral somatosensory neurons result in aberrant tactile responses and ASD-relevant behaviors in *Shank3* mutants, the neural substrates of whisker-dependent behaviors have been poorly investigated in this model.

Based on somatosensory processing deficits reported in PMS patients (Philippe et al. 2008), we hypothesized that similar abnormalities were present in *Shank3b*$^{-/-}$ mice. Thus, we investigated the neural substrates of somatosensory responses in adult *Shank3b*$^{-/-}$ and control mice. *Shank3b*$^{-/-}$ mice showed hypo-reactivity to whisker-dependent cues, accompanied by reduced expression of the immediate-early gene c-*fos* in the primary somatosensory cortex (S1) and hippocampus. Finally, we used rsfMRI to probe functional connectivity between cortico-hippocampal regions that exhibited a reduced c-*fos* response. Our results indicate that *Shank3b*$^{-/-}$ mice show hypo-connectivity within the somatosensory-hippocampal network.

Materials and methods

Animals

Animal research protocols were reviewed and approved by the University of Trento animal care committee and Italian Ministry of Health, in accordance with the Italian law (DL 26/2014, EU 63/2010). Animals were housed in a 12 h light/dark cycle with food and water available *ad libitum*. All surgical procedures were performed under anesthesia and all efforts were made to minimize suffering. *Shank3B* mutant mice were originally generated by Peça et al. (2011) by targeting the fragment encoding the PDZ domain of SHANK3. These mutants display a complete loss of both SHANK3α and SHANK3β isoforms, accompanied by a significant reduction of the putative SHANK3γ isoform. *Shank3b* mutants were purchased from The Jackson Laboratory and crossed at least five times into a C57BL/6 background. Heterozygous mating (*Shank3b*$^{+/-}$ × *Shank3b*$^{+/-}$) was used to generate the *Shank3b*$^{+/+}$ and *Shank3b*$^{-/-}$ littermates used in this study. PCR genotyping was performed according to the protocol available on The Jackson Laboratory website (www.jax.org). A total of 119 age-matched adult littermates (63 *Shank3b*$^{+/+}$ and 56 *Shank3b*$^{-/-}$; 3–6 months old; weight = 25–35 g) of both sexes were used. A total of 21 mice (11 *Shank3b*$^{+/+}$ and 10 *Shank3b*$^{-/-}$) were used for fMRI experiments and 67 mice (36 *Shank3b*$^{+/+}$ and 31 *Shank3b*$^{-/-}$) were used for behavioral testing. A subset of animals subjected to the WN test (nine *Shank3b*$^{+/+}$ and seven *Shank3b*$^{-/-}$) was used for c-*fos* mRNA in situ hybridization. An additional group of six *Shank3b*$^{+/+}$ and five *Shank3b*$^{-/-}$ mice received only sham stimulation and were used as controls for in situ hybridization experiments (no difference in WN scores was detected between genotypes in this additional group of animals). Seven mice (three stimulated and four controls) per genotype were used for the c-*fos* mRNA study following whisker stimulation under anesthesia. Finally, three mice per genotype were used for awake head-fixed whisker stimulation. Previous studies showed that similar group sizes are sufficient to obtain statistically significant results in fMRI (Haberl et al. 2015; Sforazzini et al. 2016; Pagani et al. 2019), behavioral, and in situ hybridization studies (Tripathi et al. 2009; Provenzano et al. 2014; Chelini et al. 2019). All experiments were performed blind to genotype. Animals were assigned a numerical code by an operator who did not take part in the experiments and codes were associated with genotypes only at the moment of data analysis.

Open field test

Mice were habituated to the testing arena prior to the texture discrimination assessment, during two consecutive days (Fig. 1A). During these two sessions, each animal was placed in empty arena (40 cm × 40 cm × 40 cm) and allowed to freely explore for 20 min. The walls of the arena were smooth and gray colored. Sessions were recorded and mice were automatically tracked using EthoVisionXT (Noldus). Distance traveled and time spent in center/borders were analyzed for both days of test.

Textured novel object recognition test

Whisker-mediated texture discrimination was assed as described (Wu et al. 2013), with minor modifications. Textured novel object recognition (tNORT) was performed in the same arena used for open field testing (Fig. 1A). On the third day, cylinder-shaped objects (1.5 cm radius base × 12 cm height) covered in garnet sandpaper were placed into the arena test. The grit (G) of the object (i.e., how rough the sandpaper is) was chosen according to previously published protocols (Wu et al. 2013; Domínguez-Iturza et al. 2019), to favor whisker interaction. A 120 G sandpaper (very

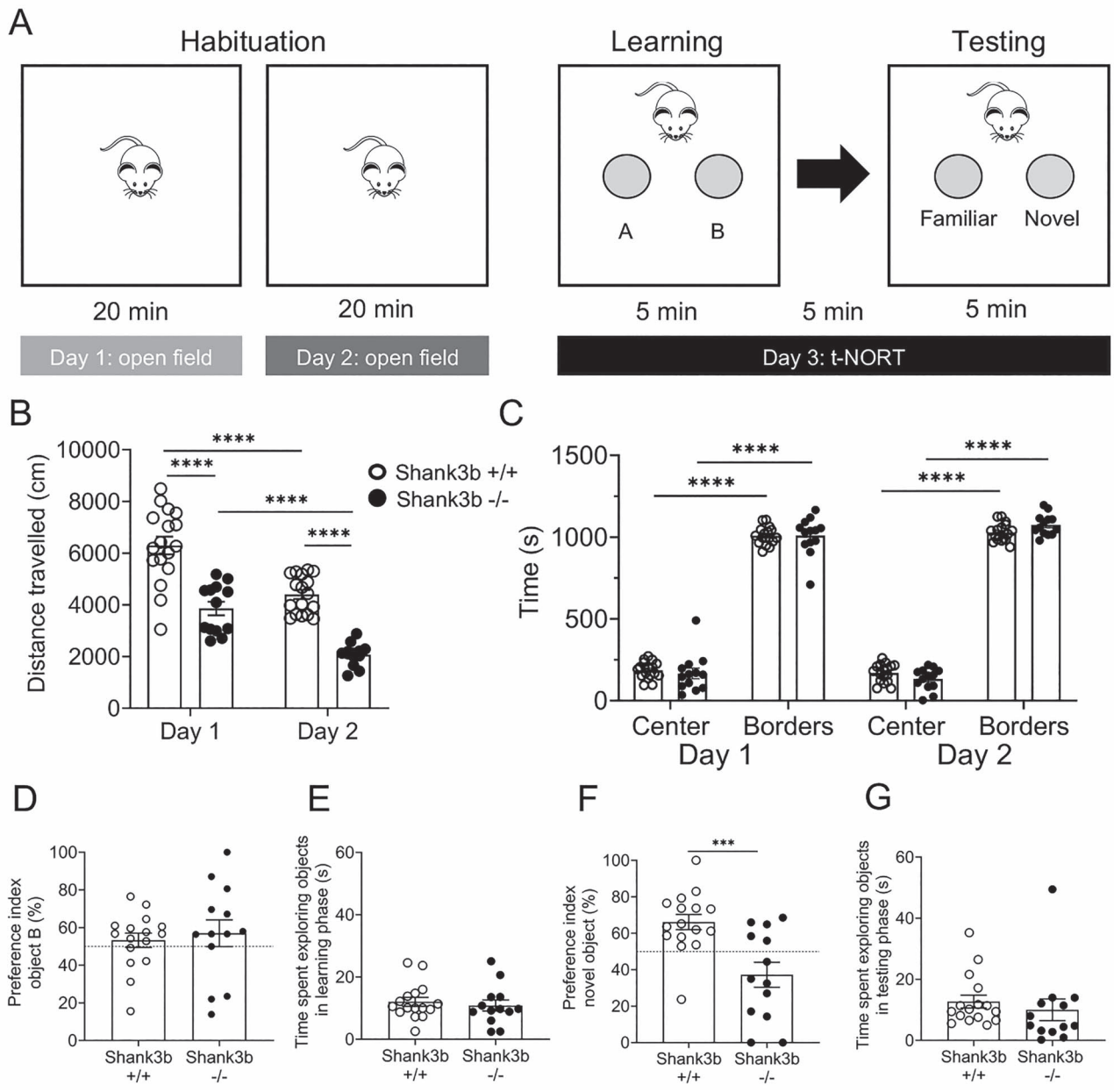

Fig. 1. *Shank3b*$^{-/-}$ mice exhibit hypo-locomotion and deficits in texture discrimination. (A) Open field and textured novel object recognition test (tNORT) experimental design. (B and C) Quantification of open field performance by *Shank3b*$^{+/+}$ and *Shank3b*$^{-/-}$ mice. *Shank3b*$^{-/-}$ mice traveled a significantly shorter distance over the two days of test, as compared to controls (B, $^{****}P < 0.0001$, Tukey's test following two-way ANOVA). Both *Shank3b*$^{+/+}$ and *Shank3b*$^{-/-}$ mice spent significantly more time in borders as compared to the center of the arena (C, $^{****}P < 0.0001$, Tukey's test following three-way ANOVA), but the time spent in center and borders did not significantly differ between genotypes (C, $P > 0.05$, Tukey's test following three-way ANOVA). (D–G) Quantification of tNORT performance by *Shank3b*$^{+/+}$ and *Shank3b*$^{-/-}$ mice. Preference index (%) for object B (D) and time spent exploring objects in learning phase (E) did not differ between *Shank3b*$^{+/+}$ and *Shank3b*$^{-/-}$ mice ($P > 0.05$, Tukey's test following two-way ANOVA). In the testing phase, *Shank3b*$^{-/-}$ mice showed a significantly lower preference index (%) for the novel object, as compared to *Shank3b*$^{+/+}$ mice (F, $^{***}P < 0.001$, Tukey's test following two-way ANOVA), while spending the same time as controls in exploring objects (G, $P > 0.05$, Tukey's test following two-way ANOVA). In D and F, the dashed line represents 50% in the preference index, meaning equal preference for both objects. See Materials and Methods for details about preference index calculation. All plots report the mean values ± SEM; each dot represents one animal. Genotypes are as indicated (n = 17 *Shank3b*$^{+/+}$ and 13 *Shank3b*$^{-/-}$ for open field; n = 16 *Shank3b*$^{+/+}$ and 13 *Shank3b*$^{-/-}$ for tNORT; one Shank3b$^{+/+}$ mouse was excluded from tNORT analysis as it did not interact with objects during the learning phase).

fine) was used for the familiar object, whereas 40 G sandpaper (very coarse) was used for the novel object. Many identical objects were created for each grit of sandpaper used in this study to avoid repetitive use of the same object across the testing period. This minimized the possibility that mice recognized one particular object using olfactory cues. In order to avoid possible visual confounders given to the different sandpaper grit, the test was performed in penumbra (4 lux). Adult mice have a very low visual acuity (Schmucker et al. 2005), which does not allow them to discriminate the grit of the two objects at this light intensity. In the first session (learning phase), mice were placed in the testing arena facing away from two identically textured

objects (object A and object B; 120 G) and allowed to freely explore the objects for 5 min. This short time was selected to favor the investigation through whiskers. The textured objects were placed in the center of the arena, equidistant to each other and the walls. Mice were then removed and held in a separate transport cage for 5 min. This short time was selected to minimize hippocampal mediated learning (Wu et al. 2013). Prior to the start of the second session, the two objects in the arena were replaced with a third, identically textured object (familiar, 120 G) and a new object with different texture (novel, 40 G). The position of the novel versus the familiar object was counterbalanced and pseudorandomized (i.e, the position of the two objects was exchanged between each mouse and the following one). Mice were then placed back into the arena for the second session (testing phase) and allowed to explore for 5 min. Since mice have an innate preference for novel stimuli, an animal that can discriminate between the textures of the objects spends more time investigating the novel textured object, whereas an animal that cannot discriminate between the textures is expected to investigate the objects equally. The testing arena was cleaned with 70% ethanol between sessions and between animals to mask olfactory cues. The amount of time mice spent actively investigating each of the objects was assessed during both learning and testing phases. Investigation was defined as directing the nose toward the object with a distance of less than 2 cm from the nose to the object or touching the nose to the object. Resting, grooming, and digging next to, or sitting on, the object was not considered as investigation. If an animal did not interact with both objects during the learning phase, it was excluded from tNORT analysis. The activity of the mice during the learning and testing phase was recorded with a video camera centered above the arena and automatically tracked using EthoVisionXT (Noldus). The performance of the mice in the tNORT was expressed by the preference index. The preference index is the ratio of the amount of time spent exploring any one of the two objects in the learning phase or the novel one in the testing phase over the total time spent exploring both objects, expressed as percentage [i.e., $A/(B + A) \times 100$ in the learning session and novel/(familiar + novel) $\times$ 100 in the testing session].

Whisker nuisance (WN) test

WN test was performed as previously described (Balasco et al. 2019; Chelini et al. 2019). Briefly, animals were allowed to habituate for 30 min to a novel empty cage (experimental cage) for 2 days before the test. To facilitate the habituation to the novel environment, home-cage bedding was placed overnight in the experimental cage and removed right before the introduction of the mouse. On test day, mice were acclimated with the experimental environment for 30 min, before the beginning of the testing phase. Testing phase was composed of four sessions, lasting 5 min each. In the first (sham) session, a wooden stick was introduced in the experimental cage, avoiding direct contact with the animal. The following three sessions consisted in stimulating mice's whiskers by continuously deflecting vibrissae using the wooden stick. To dissect the complexity of behavioral response to mechanical whisker stimulation in freely moving mice, multiple behavioral categories were identified and independently quantified by an investigator blind to the experimental conditions. The identified categories, based on a previous version of the test (Balasco et al. 2019; Chelini et al. 2019), included freezing, guarded behavior, evasion, and response to stick. Freezing was scored when the animal was immobile in a defensive posture (passive guarded behavior: curved back, protracted neck and stretched limbs, or fully hunched posture). Active guarded behavior corresponded to a defensive posture when the animal was not immobile. Evasion was defined as the active avoidance of the stick by either running in the opposite direction or walking backward while keeping eye-contact with the object. Freezing, guarded behavior, and evasion were quantified as the time spent in each behavior. Finally, response to stick was split in two sub-categories: climbing and startle. Climbing events were counted each time the animal attempted active exploration of the stick by rearing on the hindlimbs and reaching with the forelimbs; startle was defined as sudden and uncoordinated avoidance movement. Both climbing and startle were quantified as the number of events detected over the total time of observation.

Whisker stimulation under anesthesia

Mice were anesthetized with an intraperitoneal injection of urethane (20% solution in sterile double-distilled water, 1.6 g/kg body weight) and head-fixed on a stereotaxic apparatus. Urethane anesthesia was chosen as it preserves whisker-dependent activity in the somatosensory cortex (Unichenko et al. 2018). WS protocol consisted in three consecutive sessions (5 min each, with 1 min intervals) of continuous touch of the whiskers with a wooden stick (bilateral stimulation), thus reproducing the stimulation protocol used in the WN test (Chelini et al. 2019).

c-*fos* mRNA in situ hybridization

Mice were killed 20 min after the end of either sham, WN, anesthesia, WS, and head-fixed whisker stimulation and brains were rapidly frozen on dry ice. Coronal cryostat sections (20 μm thick) were fixed in 4% paraformaldehyde and processed for nonradioactive in situ hybridization (Bozzi et al. 2000; Tripathi et al. 2009) using a digoxigenin-labeled c-*fos* riboprobe. Signal was detected by alkaline phosphatase-conjugated antidigoxigenin antibody followed by alkaline phosphatase staining. Brain slices from different experimental paradigms were processed together for c-*fos* mRNA expression in order to exclude possible batch effects. Sense riboprobes, used as negative control, revealed no detectable signal (data not shown). Digital images from four to eight sections

per animal were acquired at the level of the S1/dorsal hippocampus using a Zeiss AxioImager II microscope at 10× primary magnification. Since we could not exclude that in freely moving mice subjected to WN c-*fos* mRNA induction occurred in S1 subfields different from the whisker-specific one, the signal was quantified in the whole S1 and not only in the barrel cortex. For consistency, the same quantification was performed following whisker stimulation under anesthesia and in head-fixed awake animals. Brain areas were identified according to the Allen Mouse Brain Atlas (https://mouse.brain-map.org).

Behavioral and in situ hybridization data analysis

Statistical analyses of behavioral and in situ hybridization data were performed with GraphPad Prism 8.0 software, with the level of significance set at $P < 0.05$. For behavioral experiments, statistical analysis was performed by two-way analysis of variance (ANOVA) followed by Tukey's or Bonferroni's post hoc test for multiple comparisons as appropriate. Three-way ANOVA followed by Tukey's post hoc test was used to quantify open field data. Kolmogorov–Smirnov and unpaired t-test were also used for two groups comparisons. To quantify c-*fos* mRNA signal intensity, acquired images were converted to 8-bit (gray-scale), inverted, and analyzed using the ImageJ software (https://imagej.net/Downloads). Mean signal intensity was measured in different counting areas drawn to identify S1 cortical layers, hippocampal subfields and other areas of interest. Mean signal intensity was divided by the background calculated in layer 1. Statistical analysis was performed by unpaired t-test or one-way ANOVA followed by Tukey's for post hoc multiple comparisons as appropriate.

Resting-state functional MRI

Data collection

Resting-state functional MRI (rsfMRI) time series acquisition in adult male *Shank3b*$^{+/+}$ (n = 11) and *Shank3b*$^{-/-}$ (n = 10) mice has been previously described (Pagani et al. 2019). All functional connectivity analyses reported here were carried out on the rsfMRI scans acquired for the Pagani et al. (2019) study. The protocol for animal preparation employed was detailed in our previous studies (Bertero et al. 2018; Liska et al. 2018; Pagani et al. 2019; Pagani et al. 2021). Briefly, animals were anesthetized with isoflurane (5% induction), intubated and artificially ventilated (2% maintenance). After surgery, isoflurane was discontinued and replaced with halothane (0.7%). Recordings started 45 min after isoflurane cessation. Functional scans were acquired with a 7 T MRI scanner (Bruker Biospin, Milan, Italy) using a 72-mm birdcage transmit coil and a 4-channel solenoid coil for signal reception. For each animal, in vivo anatomical images were acquired with a fast spin echo sequence (repetition time [TR] = 5500 ms, echo time [TE] = 60 ms, matrix 192 × 192, field of view 2 × 2 cm, 24 coronal slices, slice thickness 500 μm). Cocenterd single-shot BOLD rsfMRI time series were acquired using an echo planar imaging (EPI) sequence with the following parameters: TR/TE 1200/15 ms, flip angle 30°, matrix 100 × 100, field of view 2 × 2 cm, 24 coronal slices, slice thickness 500 μm for 500 volumes.

Functional connectivity data analysis

Before mapping rsfMRI connectivity, raw data were preprocessed and denoised as previously described (Sforazzini et al. 2016; Michetti et al. 2017; Liska et al. 2018). First, the initial 50 volumes were removed to allow for T1 equilibration effects. Time series were then despiked, motion corrected and registered to a common reference template. Motion traces of head realignment parameters and mean ventricular signal were then used as nuisance covariates and regressed out from each time course. Before functional connectivity mapping, all time-series underwent also band-pass filtering (0.01–0.1 Hz) and spatial smoothing (FWHM = 0.6 mm). Target regions of long-range connectivity alterations in *Shank3b*$^{-/-}$ mice were mapped using seed-based analysis. Specifically, bilateral seeds of 3 × 3 × 1 voxels were placed in the dorsal hippocampus, S1, and ventral posteromedial nucleus of the thalamus (VPM) of *Shank3b*$^{+/+}$ and *Shank3b*$^{-/-}$ mice to probe impaired functional connectivity between these regions and the rest of the brain. The location of the bilateral seeds employed for mapping are indicated in Figures 5 and 6. Functional connectivity was measured with Pearson's correlation and *r*-scores were transformed to z-scores using Fisher's *r*-to-z transform before statistics. Voxel-wise intergroup differences for seed-based mapping were assessed using a two-tailed Student's t-test ($|t| > 2$, $P < 0.05$) and family-wise error (FWER) cluster-corrected using a cluster threshold of $P = 0.01$. To quantify rsfMRI alterations we also carried out functional connectivity measures in cubic regions of interest (3 × 3 × 1 voxels). The statistical significance of these region-wise intergroup effects was quantified using a two-tailed Student's *t*-test ($|t| > 2$, $P < 0.05$).

Results

Shank3b$^{-/-}$ mice show aberrant texture discrimination through whiskers

Human research suggests that PMS is associated with aberrant sensory responses. To test the presence of a similar dysfunction in *Shank3* mutant mice, we first tested *Shank3b*$^{-/-}$ and control mice in a whisker-dependent version of tNORT (Wu et al. 2013) (Fig. 1A) using sandpaper-wrapped cylinders that differ only in texture (smooth or rough; see Materials and Methods). As a general measure of locomotor activity and generalized anxiety we first assessed *Shank3b*$^{-/-}$ and control mice in an open field arena in two consecutive days. During both days of testing, *Shank3b*$^{-/-}$ mice showed a significantly reduced distance traveled (Fig. 1B; two-way ANOVA, *Shank3b*$^{+/+}$ vs. *Shank3b*$^{-/-}$; main effect

of genotype $F_{(1, 56)} = 86.93$; $P < 0{,}0001$; main effect of testing days $F_{(1, 56)} = 52.05$, $P < 0{,}0001$; post hoc Tukey's test, *Shank3b*$^{+/+}$ vs. *Shank3b*$^{-/-}$ within day 1 and 2, $P < 0.0001$) and time spent moving (Supplementary Fig. 1) compared to control littermates. Both genotypes showed a significant reduction of distance traveled (Fig. 1B; Tukey's post hoc following two-way ANOVA, *Shank3b*$^{+/+}$ day 1 vs. *Shank3b*$^{+/+}$ day 2 and *Shank3b*$^{-/-}$ day 1 vs. *Shank3b*$^{-/-}$ day 2; $P < 0.0001$) and time spent moving (Supplementary Fig. 1) between testing days, indicating habituation to the novel environment. Both genotypes also spent a comparable amount of time in center and borders of the open field arena (Fig. 1C) over the two days of habituation (three-way ANOVA, *Shank3b*$^{+/+}$ vs. *Shank3b*$^{-/-}$; main effect of genotype $F_{(1, 112)} = 0.03368$, $P = 0.8547$; main effect of days $F_{(1, 112)} = 0.4418$, $P = 0.5076$; main effect of arena regions $F_{(1, 112)} = 4081$, $P < 0{,}0001$). Finally, both *Shank3b*$^{-/-}$ and control mice displayed a preference for borders regions of the arena during both days of testing (Fig. 1C; Tukey's post hoc following three-way ANOVA, center vs. borders within *Shank3b*$^{+/+}$ and center vs. borders within *Shank3b*$^{-/-}$; $P < 0.0001$), indicating a similar anxious behavior in both genotypes.

During the tNORT learning phase (Fig. 1D) both genotypes did not show any preference for one of the identical textured objects (unpaired t-test, *Shank3b*$^{+/+}$ vs. *Shank3b*$^{-/-}$, $P = 0.6219$). During the test phase, control mice spent a significantly larger amount of time exploring the novel object, testifying a preference in the novelty exploration through whiskers. Conversely, *Shank3b*$^{-/-}$ mice spent comparable time exploring the novel and the old object, (Fig. 1F; unpaired t-test, *Shank3b*$^{+/+}$ vs. *Shank3b*$^{-/-}$, $P = 0.0008$; see also Supplementary Fig. 2). Moreover, the amount of time spent investigating objects during both learning and testing phase did not differ between genotypes (unpaired t-test, *Shank3b*$^{+/+}$ vs. *Shank3b*$^{-/-}$; $P > 0.05$; Fig. 1E and G), indicating that mutant mice did not exhibit an aversion to the objects, and did not avoid object exploration through whiskers. In keeping with the open field data, *Shank3b*$^{-/-}$ mice showed a significantly lower distance traveled and velocity in the tNORT test (Supplementary Fig. 3). These results indicate that *Shank3b*$^{-/-}$ mice show aberrant whisker-dependent texture discrimination.

Shank3b$^{-/-}$ mice display hypo-reactivity to repetitive whisker stimulation

We next used the whisker nuisance test (WN; Balasco et al. 2019, Chelini et al. 2019) to assess the behavioral responses to whisker stimulation in freely moving *Shank3b*$^{-/-}$ and control mice. *Shank3b*$^{-/-}$ and control mice were repetitively stimulated with a wooden stick over three sequential trial sessions of 5 min each following a sham session that allowed to set the baseline of behavioral responses (Fig. 2A). Four different behavioral responses (freezing, guarded behavior, evasion, and response to stick) were quantified (see Materials and Methods). Two-way ANOVA revealed a significant effect of trial for all behaviors analyzed (main effect of trial $F_{(3, 140)} = 14{,}83$ for freezing; $F_{(3, 140)} = 14{,}12$ for guarded; $F_{(3, 140)} = 22{,}06$ for evading; $F_{(3, 140)} = 46{,}09$ for climbing; $F_{(3, 140)} = 12{,}60$ for startle; $P < 0.0001$; Figure 2B–E and data not shown), and a significant effect of genotype for evading, climbing, and startle behaviors (main effect of genotype $F_{(1, 140)} = 8{,}33$ for evading; $F_{(1, 140)} = 9{,}49$ for climbing; $F_{(1, 140)} = 6{,}98$ for startle; $P < 0.01$; Figure 2D, E and data not shown). Overall, the behavioral responses of *Shank3b*$^{+/+}$ and *Shank3b*$^{-/-}$ mice did not differ during the pre-stimulation (sham) session, with the two genotypes showing comparable guarded and evading behaviors when the stick was presented in proximity of the animal's head, avoiding any contact (Kolmogorov–Smirnov test; *Shank3b*$^{+/+}$ vs. *Shank3b*$^{-/-}$, $P > 0.05$; Fig. 2C-E and Supplementary Table 3). Climbing and startle responses to stick were absent in both genotypes during the sham session. However, *Shank3b*$^{-/-}$ mice displayed significantly longer freezing during the sham session compared with controls (Kolmogorov–Smirnov test, *Shank3b*$^{+/+}$ vs. *Shank3b*$^{-/-}$; $P = 0.006$; Fig. 2B and Supplementary Table 3). Importantly, *Shank3b*$^{+/+}$ and *Shank3b*$^{-/-}$ mice spent a comparable time moving during the sham session (*Shank3b*$^{+/+}$: $176{,}7 \pm 10{,}47$ s; *Shank3b*$^{-/-}$: $171{,}3 \pm 13{,}76$ s; Kolmogorov–Smirnov test; $P = 0{,}9162$). In the first trial, both genotypes exhibited significantly higher scores in freezing, guarded, and evading behaviors compared to the sham session, indicating a similar fearful response to whisker stimulation (Bonferroni's test following two-way ANOVA; trial 1 vs. sham within *Shank3b*$^{+/+}$ and *Shank3b*$^{-/-}$, $P < 0.05$; Fig. 2B–D). However, *Shank3b*$^{-/-}$ mice spent significantly less time in evasion compared to *Shank3b*$^{+/+}$ controls, while no difference was observed in freezing and guarded behaviors during trial 1 (Kolmogorov–Smirnov test; *Shank3b*$^{+/+}$ vs. *Shank3b*$^{-/-}$ within trial 1, $P < 0.05$ for evading, $P > 0.05$ for freezing and guarded; Fig. 2B–D and Supplementary Table 3). Both genotypes exhibited a significant reduction in freezing, guarded, and evading behaviors from the first to the third trial, indicating habituation to repetitive whisker stimulation (Bonferroni's test following two-way ANOVA; trial 3 vs. trial 1 within *Shank3b*$^{+/+}$ and *Shank3b*$^{-/-}$; $P < 0.05$ for all behaviors; Fig. 2B–D). Moreover, *Shank3b*$^{-/-}$ mice displayed significantly impaired curiosity toward the stimulus, as indicated by their fewer climbing events compared to controls during trial 3 (Kolmogorov–Smirnov test; *Shank3b*$^{+/+}$ vs. *Shank3b*$^{-/-}$ within trial 3, $P = 0.004$; Fig. 2E and Supplementary Table 3). Finally, no major differences in behavioral scores were observed between sexes within the two genotypes, with few exceptions (see Supplementary Table 4 for details and statistical analyses). These findings indicate that *Shank3b*$^{-/-}$ mice are less prone to engage in proactive behaviors in response to invasive whisker stimulation compared to control animals. Thus, lack of *Shank3b* does not affect the ability of experiencing fear, but drastically disrupts the way the animal responds to a novel and invasive stimulus.

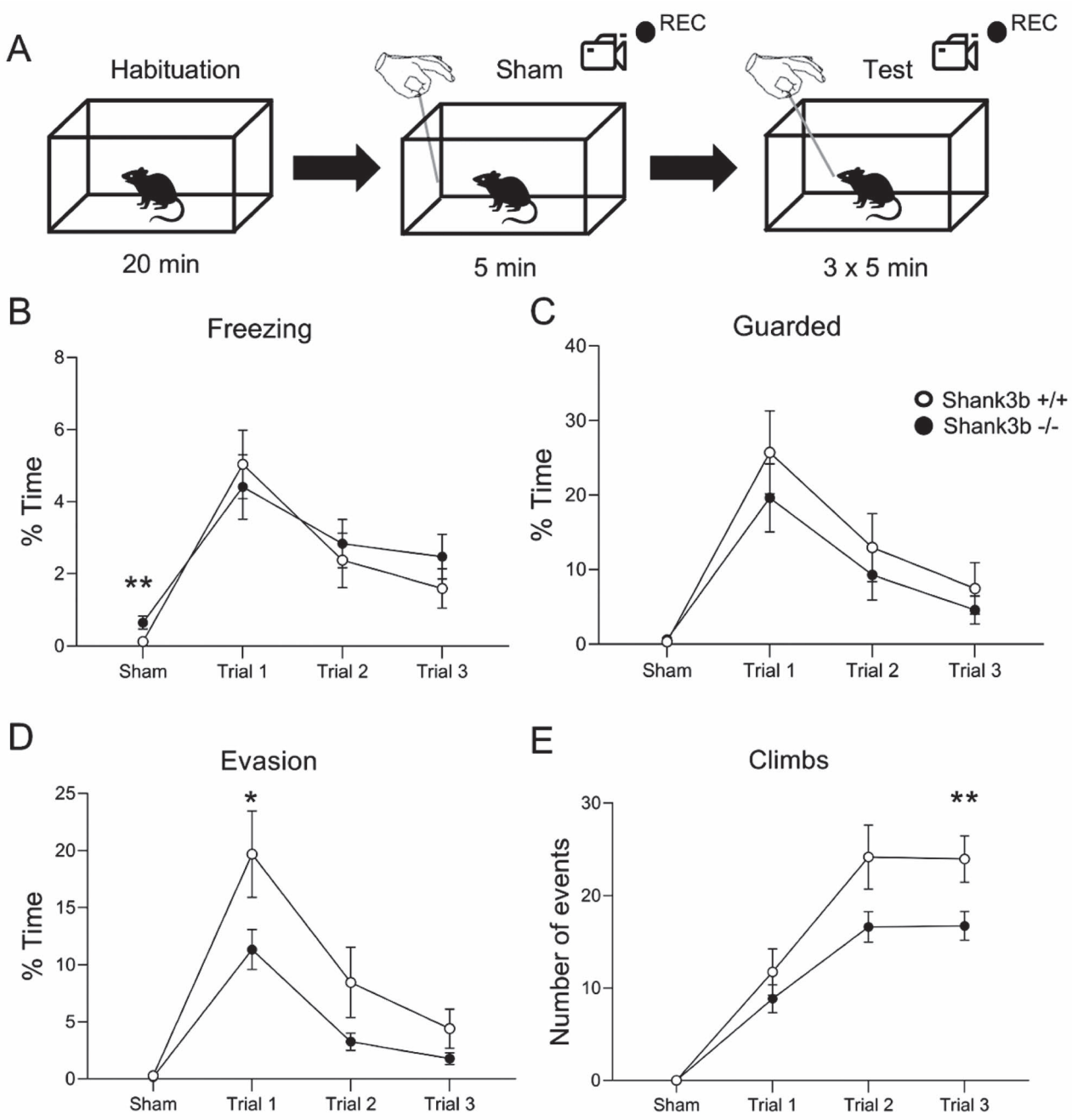

Fig. 2. *Shank3b*$^{-/-}$ mice display reduced evading and exploratory behaviors following repetitive whisker stimulation in WN. (A) WN experimental design; four different parameters (freezing, guarded behavior, evasion, and climbing in response to stick presentation) were monitored across the sham session (no tactile stimulation) and three different experimental trials of repetitive whisker stimulation (see Materials and Methods for details). (B–D) Time spent in freezing (B), guarded behavior (C), and evading (D), expressed as % over the total time of observation in each session (sham and trials 1–3). (E) Number of climbing events in response to stick presentation, expressed as the total number of events during each session (sham and trials 1–3). All plots report mean values ± SEM. *$P < 0.05$, **$P < 0.01$, Komogorov–Smirnov test. Genotypes are as indicated (n = 19 *Shank3b*$^{+/+}$ and 18 *Shank3b*$^{-/-}$).

Shank3b$^{-/-}$ mice lack c-*fos* mRNA induction in S1 and hippocampus following repetitive whisker stimulation

Shank3b$^{-/-}$ mice sensory hypo-responsiveness in the WN task led us to investigate the neural substrates of aberrant whisker-dependent behaviors in these mutants. To this aim, we used c-*fos* mRNA expression as a molecular proxy for neural activity (Filipkowski et al. 2000; Chelini et al. 2019) and quantified in situ hybridization signal intensity in multiple regions of *Shank3b*$^{-/-}$ and control brains 20 min after either a sham or WN session. Comparable expression of c-*fos* mRNA was observed in both genotypes following the sham session (Fig. 3A and B, Supplementary Table 5). Conversely, while WN induced a significant upregulation of c-*fos* mRNA in *Shank3b*$^{+/+}$ S1 (Fig. 3A and Supplementary Fig. 4), no difference between sham and WN mice was detected in *Shank3b*$^{-/-}$ mice in the same area (Fig. 3C; Tukey's post hoc following one-way ANOVA, Sham vs. WN in *Shank3b*$^{+/+}$ $P < 0.0001$). c-*fos* mRNA levels in the hippocampus did not differ

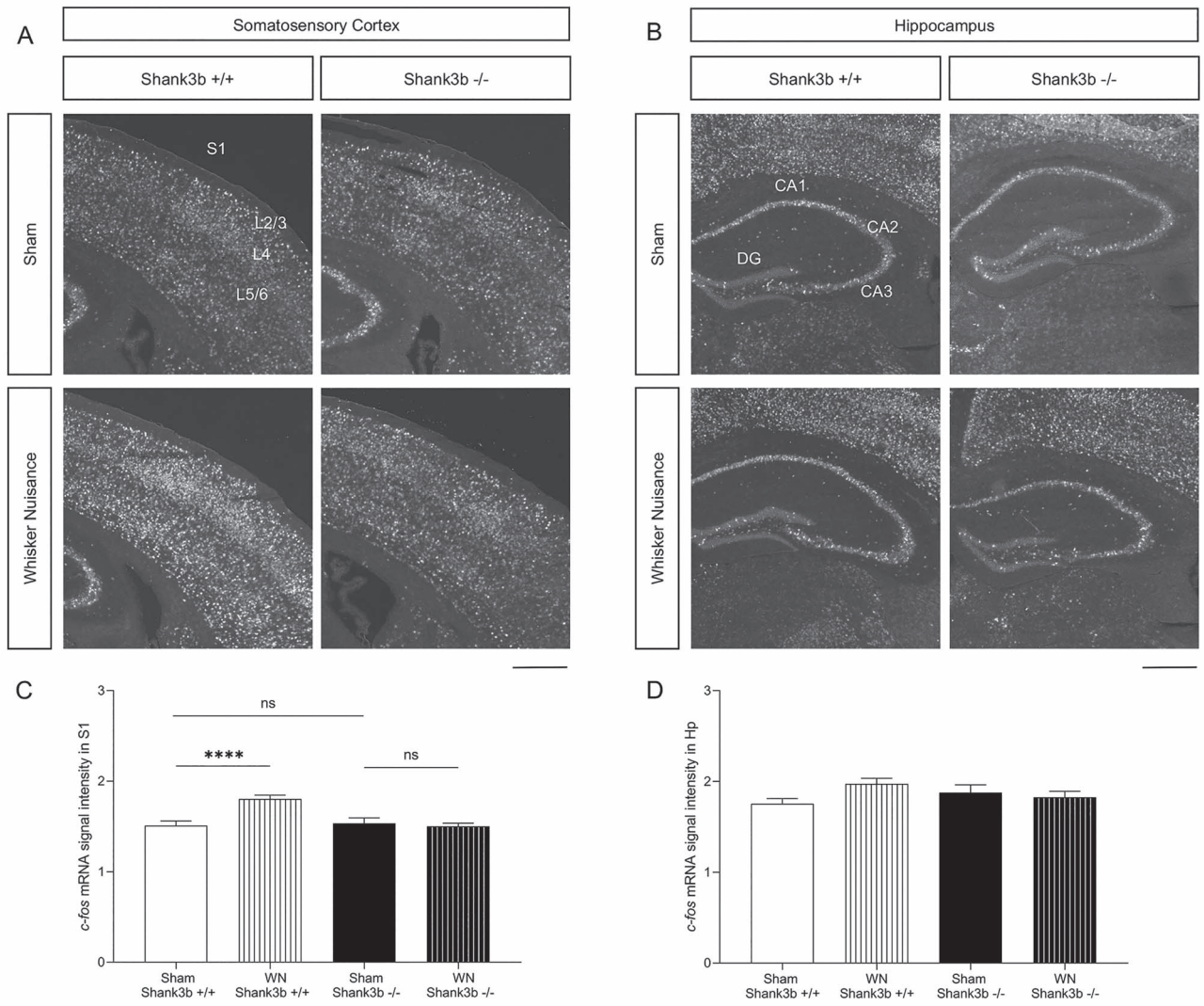

Fig. 3. *Shank3b*$^{-/-}$ mice lack c-*fos* mRNA induction in S1 and following WN. (A, B). Representative images of c-*fos* mRNA in situ hybridization in S1 and hippocampus of *Shank3b*$^{+/+}$ and *Shank3b*$^{-/-}$ mice, 20 min following sham or WN. Scale bars, 500 μM. (C) Quantification of c-*fos* mRNA signal intensity in S1 following sham and WN. (D) Quantification of c-*fos* mRNA signal intensity in the hippocampus following sham and WN. Values are expressed as mean signal intensities ±SEM (see Materials and Methods). ****$P < 0.0001$, Tukey post hoc test following one-way-ANOVA (n = 44 sections from nine *Shank3b*$^{+/+}$ mice and 40 sections from seven *Shank3b*$^{-/-}$ mice following WN and n = 43 sections from six *Shank3b*$^{+/+}$ mice and 37 sections from five *Shank3b*$^{-/-}$ mice following sham). Genotypes and treatments are as indicated. Abbreviations: CA1/2/3, hippocampal pyramidal cell layers; DG, dentate gyrus; Hp, hippocampus; L2–6, S1 cortical layers; S1, primary somatosensory cortex.

between sham and WN animals in both genotypes (Fig. 3B, D; $P > 0.05$, one-way ANOVA). No difference in c-*fos* mRNA expression was detected between the two genotypes in other brain regions analyzed, including the motor cortex (Supplementary Fig. 5).

We next investigated c-*fos* mRNA induction following whisker stimulation (WS) in lightly anesthetized *Shank3b*$^{+/+}$and *Shank3b*$^{-/-}$ mice. In situ hybridization experiments showed comparable levels of c-*fos* mRNA in S1 and hippocampus in both genotypes following anesthesia only (Fig. 4A, B and Supplementary Table 6). WS resulted in marked induction of c-*fos* mRNA in S1 (Fig. 4A) and hippocampus (Fig. 4B) of *Shank3b*$^{+/+-}$ but not *Shank3b*$^{-/-}$ mice, as compared to anesthetized unstimulated controls. Quantification of c-*fos* mRNA signal intensity confirmed these findings (Fig. 4C and D; Tukey's post hoc following one-way ANOVA; anesthesia vs. WS $P < 0.0001$ in Shank3b$^{+/+}$ S1 and hippocampus; see also Supplementary Fig. 6). WS also induced a significant c-*fos* mRNA upregulation in the somatosensory thalamus (VPM, ventral posterior medial nucleus, which receives afferents from whiskers via brainstem nuclei and projects to S1 layer 4; Petersen 2007) and amygdala of *Shank3b*$^{+/+}$ but not *Shank3b*$^{-/-}$ mice, as compared to anesthetized unstimulated controls (Supplementary Fig. 7C and D). No difference in c-*fos* mRNA expression was detected between the two genotypes in other brain regions analyzed (Supplementary Fig. 7A and B).

To further investigate the whisker-dependent responses of the same brain areas, we next performed a protocol of automated unilateral whisker stimulation in head-fixed awake animals. We found a significant upregulation of c-*fos* mRNA in the stimulated S1

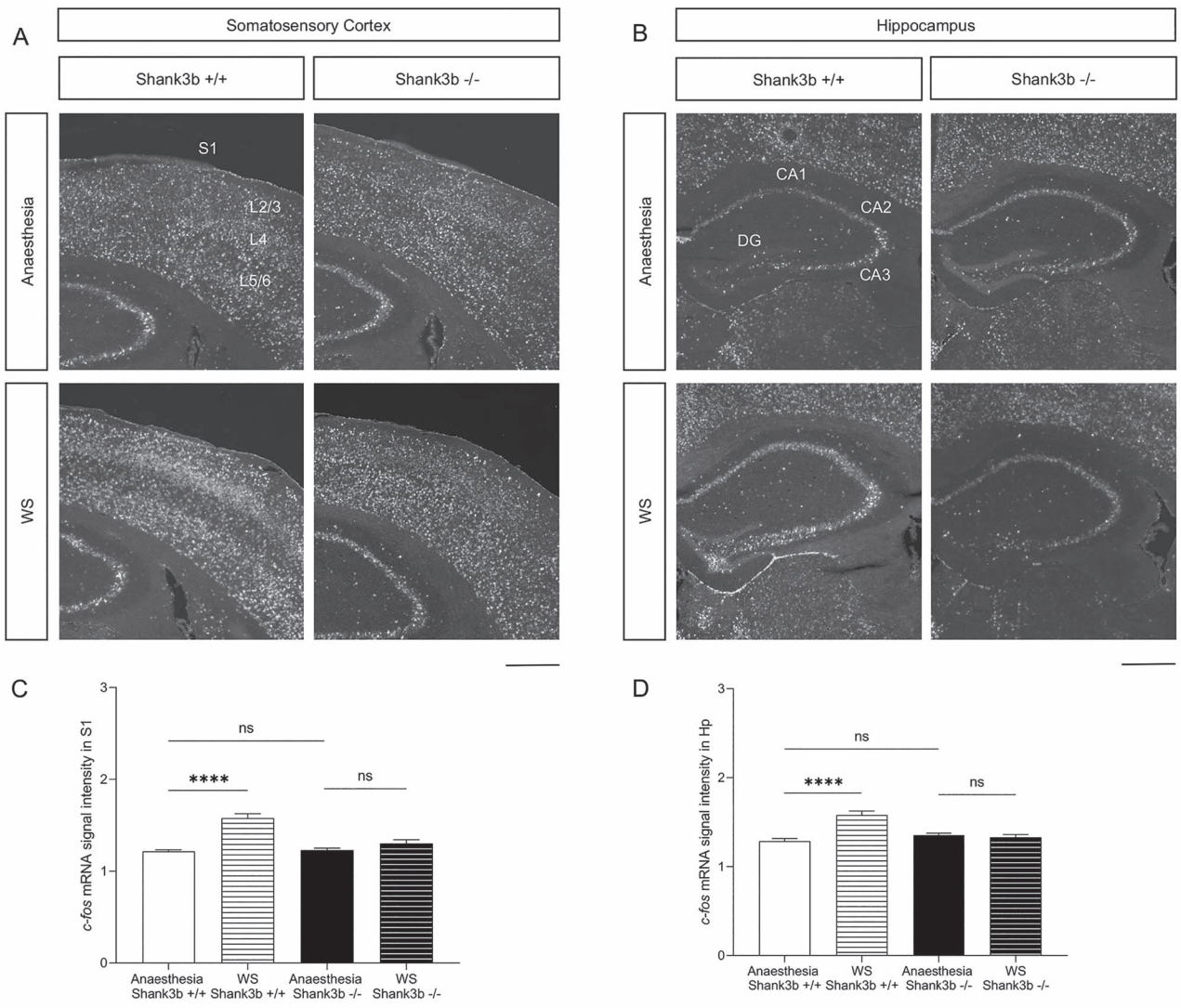

Fig. 4. *Shank3b*$^{-/-}$ mice lack c-*fos* mRNA induction in S1 and following whisker stimulation under anesthesia. (A, B) Representative images of c-*fos* mRNA in situ hybridization in the primary somatosensory cortex (A) and hippocampus (B) of *Shank3b*$^{+/+}$ and *Shank3b*$^{-/-}$ mice, 20 min following anesthesia or whisker stimulation under anesthesia. Scale bars, 500 μm. (C, D) Quantification of c-*fos* mRNA signal intensity in S1 (C) and hippocampus (D) of *Shank3b*$^{+/+}$ and *Shank3b*$^{-/-}$ mice. Values are expressed as mean normalized signal intensities ±SEM. ****$P < 0.0001$ Tukey post hoc test following one-way-ANOVA (n = 19 sections from three *Shank3b*$^{+/+}$ mice and 18 sections from three *Shank3b*$^{-/-}$ mice following WS and n = 30 sections from four *Shank3b*$^{+/+}$ mice and 32 sections from four *Shank3b*$^{-/-}$ mice following anesthesia). Genotypes and treatments are as indicated. Abbreviations: CA1/2/3, hippocampal pyramidal cell layers; DG, dentate gyrus; Hp, hippocampus; L2–6, S1 cortical layers; S1, primary somatosensory cortex.

(contralateral to whisker stimulation) of both genotypes (Supplementary Fig. 8A and B; Tukey's post hoc following one-way ANOVA, Stim vs. No Stim $P < 0.0001$ in *Shank3b*$^{+/+}$ and $P = 0.0008$ in *Shank3b*$^{-/-}$). However, c-*fos* mRNA induction in the stimulated S1 was lower in *Shank3b*$^{-/-}$ mice compared to *Shank3b*$^{+/+}$ controls (Supplementary Fig. 8B; Tukey's post hoc following one-way ANOVA, *Shank3b*$^{+/+}$ Stim vs. *Shank3b*$^{-/-}$ Stim $P = 0.0128$). No differences were found between non-stimulated S1 (ipsilateral to whisker stimulation) of both genotypes (Supplementary Fig. 8A, B; Tukey's post hoc following one-way ANOVA, *Shank3b*$^{+/+}$ No Stim vs. *Shank3b*$^{-/-}$ No Stim, $P = 0.0906$). Moreover, quantification of c-*fos* mRNA in the hippocampus revealed a significantly reduced activation in stimulated *Shank3b*$^{-/-}$ compared to stimulated *Shank3b*$^{+/+}$ controls (Supplementary Fig. 8C and D; unpaired t-test $P = 0.0001$). No difference in c-*fos* expression was detected between the two genotypes in other brain regions analyzed (Supplementary Fig. 8E–H and Supplementary Table 7).

These findings indicate that in *Shank3b*$^{-/-}$ mice, whisker stimulation does not result in c-*fos* mRNA induction in both S1 and hippocampus, suggesting an impaired crosstalk between these two areas in *Shank3b* mutants.

Reduced long-range functional connectivity between hippocampus and S1 in *shank3b*$^{-/-}$ mice

We previously showed that loss of *Shank3b* leads to profoundly altered cortico-cortical functional coupling

(Pagani et al. 2019). To investigate whether the regional deficits observed upon repetitive whisker stimulation could be linked to similarly impaired hippocampus-S1 functional synchronization, we probed rsfMRI connectivity of the dorsal hippocampus, a brain region characterized by a decreased c-*fos* signal in *Shank3b* mutants (Figs 3 and 4). Interestingly, rsfMRI mapping revealed markedly reduced functional connectivity between the dorsal hippocampus and S1 ($|t| > 2$, $P < 0.05$ and FWER cluster-corrected using a cluster threshold of $P = 0.01$, Fig. 5A). Quantification of rsfMRI signal in regions of interest confirmed impaired functional connectivity between hippocampus and S1 ($t = 3.57$, $P = 0.002$, Fig. 5B), which, like the dorsal hippocampus, we found not to be activated by sensory stimuli in *Shank3b*$^{-/-}$ mice (Figs 3, 4 and Supplementary Fig. 8). To rule out the presence of connectivity alterations between VPM and S1, and between these two regions and the brainstem trigeminal nucleus (TN), we then carried out seed-based connectivity analysis of the VPM and S1. Seed-based mapping of VPM revealed preserved rsfMRI connectivity with S1 and trigeminal nucleus in *Shank3b*$^{-/-}$ mice ($|t| > 2$, $P < 0.05$ and FWER cluster-corrected using a cluster threshold of $P = 0.01$, Fig. 6A). Similarly, seed-based mapping of the S1 revealed preserved rsfMRI connectivity with VPM and TN in *Shank3b*$^{-/-}$ mice ($|t| > 2$, $P < 0.05$ and FWER cluster-corrected using a cluster threshold of $P = 0.01$, Fig. 6B). The presence of unaltered rsfMRI connectivity between the VPM and S1 was confirmed by quantifications in regions of interest ($t = 0.68$, $P = 0.50$, Fig. 6C). These findings suggest that the reduced cortical-hippocampal response observed in *Shank3b* mutants might specifically result from a weakened functional coupling between hippocampal and somatosensory areas.

Discussion

In this study, we report that *Shank3b* mutant mice display aberrant whisker-dependent behaviors. This trait is associated with altered response and coupling of circuits involved in sensory processing. Specifically, we found that *Shank3b*$^{-/-}$ adult mice showed normal exploration through whiskers but reduced texture discrimination in a whisker-dependent task. *Shank3b*$^{-/-}$ mice showed hypo-responsiveness to repetitive whisker stimulation, accompanied by a significantly reduced c-*fos* mRNA induction in S1 and hippocampus. Finally, using rsfMRI, we detected decreased long-range functional connectivity between hippocampus and S1 in mutant mice, but preserved functional coupling between S1 and somatosensory areas of the thalamus and brainstem. We propose that hypo-connectivity and reduced activation of cortico-hippocampal circuits might represent a functional substrate for hypo-reactivity to whisker-dependent cues in *Shank3b*$^{-/-}$ mice.

Previous studies investigated tactile discrimination in mouse strains harboring ASD-related mutations, including *Shank3b* mutants (Orefice et al. 2016; Orefice et al. 2019). In these investigations, tNORT was performed after whisker removal to avoid whisking investigations and promote object exploration via paws' glabrous skin. The reported results suggest that whisker-independent aberrant texture discrimination is a common trait in ASD mouse models (Orefice et al. 2016; Orefice et al. 2019; Orefice 2020). Mice use their whiskers to explore and navigate the surrounding environment (Ahl 1986; Brecht 2007; Diamond et al. 2008; Diamond and Arabzadeh 2013). Interestingly, whisker-dependent responses are affected in mouse strains bearing mutations in ASD-relevant genes (He et al. 2017; Chelini et al. 2019; Balasco et al. 2020; Chen et al. 2020; Pizzo et al. 2020). Here we sought to investigate the neural substrates of whisker-dependent behaviors in *Shank3b*$^{-/-}$ adult mice. We first used a version of tNORT specifically designed to favor whisker-mediated object exploration (see and Materials and Methods) (Wu et al. 2013). In this task, the majority (8 out of 13; 61%) of *Shank3b*$^{-/-}$ mice spent significantly less time exploring the novel (differently textured) object than control mice (Fig. 1F). However, some *Shank3b*$^{-/-}$ mice (5 out of 13, 39%) spent about 60% of their time exploring the novel object (Fig. 1F), indicating a certain variability in texture-dependent discrimination in these mutants. Together, these results indicate that *Shank3b*$^{-/-}$ mice do not avoid object interaction through whiskers, yet showing aberrant whisker-dependent texture discrimination. We cannot exclude the possibility that their hypo-locomotor phenotype (Fig. 1B) partially affects whisker-guided exploration, as suggested by the reduced distance traveled and velocity in both learning and testing phases of the tNORT (Supplementary Fig. 3). However, *Shank3b*$^{-/-}$ mice spent the same amount of time investigating objects as controls (Fig. 1E and G).

We next asked whether *Shank3b*$^{-/-}$ mice are less prone to engage in proactive behaviors in response to novelty or threats. We thus used the WN test to study *Shank3b*$^{-/-}$ mice behavior in response to active whisker stimulation. This test has been recently used to characterize whisker-dependent behaviors in mice harboring ASD-relevant mutations (Chelini et al. 2019; Pizzo et al. 2020). Here we used a quantitative approach to score behavioral responses to stimulus presentation (freezing, guarded, evading, and stick-climbing behaviors). *Shank3b*$^{-/-}$ mice displayed a significantly reduced avoidance behavior in the WN test, as indicated by their lower score in the evasion and climbing categories (Fig. 2D and E). During the sham session, both genotypes showed comparable responses in evading, guarded, and climbing behavior (Fig. 2C-E), while *Shank3b*$^{-/-}$ mice displayed significantly more freezing (Fig. 2B). Both genotypes showed a comparable fear response (freezing and guarded behaviors) to repetitive whisker stimulation (Fig. 2B and C), suggesting that anxiety does not affect mice's performance in the WN test. Finally, we detected no major differences in behavioral scores between male and female mice of both genotypes (Supplementary Table 4), in line with other

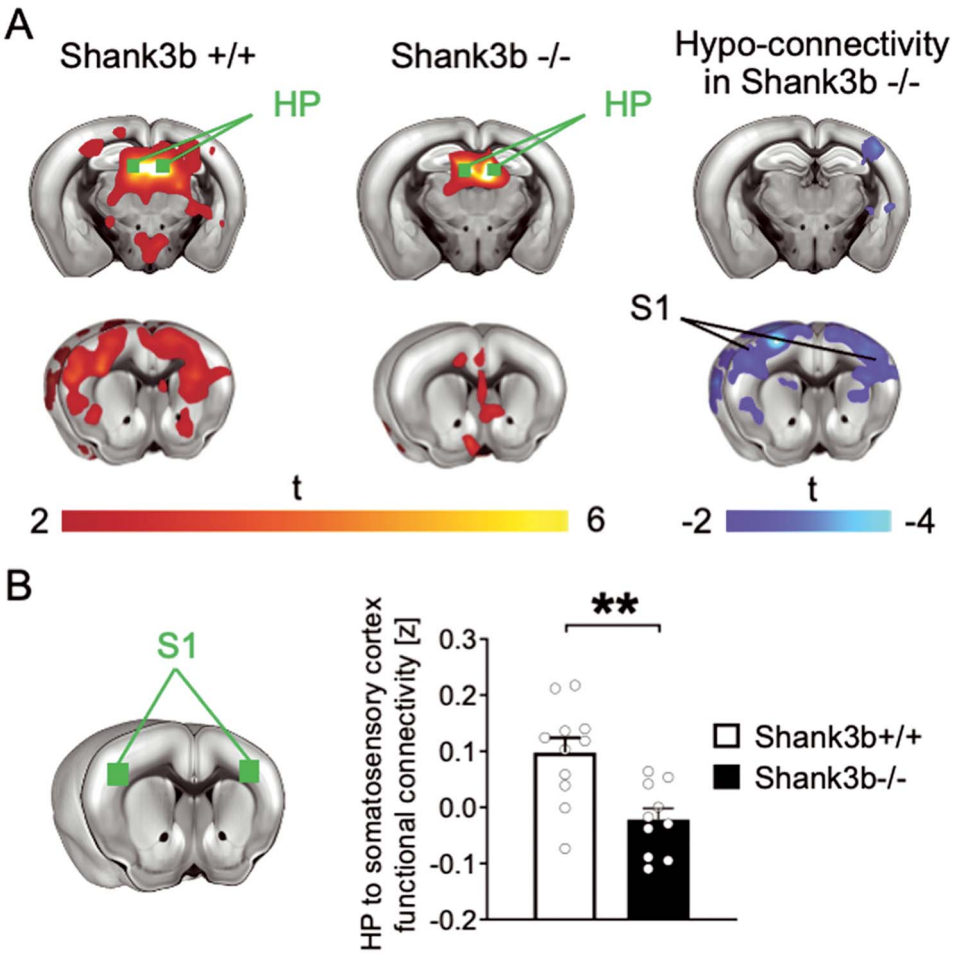

Fig. 5. Impaired functional connectivity between hippocampus and primary somatosensory cortex (S1) in *Shank3b*$^{-/-}$ mice. (A) Seed-based connectivity maps of the dorsal hippocampus in *Shank3b*$^{+/+}$ and *Shank3b*$^{-/-}$ mice. Red-yellow represents brain regions showing significant rsfMRI functional connectivity with the dorsal hippocampus (HP) in *Shank3b*$^{+/+}$ (left) and *Shank3b*$^{-/-}$ mice (middle). Seed region is depicted in green. Brain regions showing significantly reduced rsfMRI connectivity in *Shank3b*$^{-/-}$ mutants with respect to *Shank3b*$^{+/+}$ control littermates are depicted in blue/light blue (right). (B) Functional connectivity was also quantified in reference volumes of interest (green) placed in S1. Error bars represent SEM. $^{**}P < 0.01$ (unpaired t-test, n = 11 *Shank3b*$^{+/+}$ and 10 *Shank3b*$^{-/-}$; each dot represents one animal). Genotypes are as indicated.

behavioral studies previously performed (Angelakos et al. 2019; Orefice et al. 2019). As discussed for the tNORT experiment, we cannot completely rule out that behavioral hypo-reactivity of *Shank3b*$^{-/-}$ mice in the WN test is partially due to their hypo-locomotor phenotype. However, it is important to point out that *Shank3b*$^{+/+}$ and *Shank3b*$^{-/-}$ mice spent a comparable time moving during the sham session, and no differences were detected in motor cortex activation between the two genotypes post WN (Supplementary Fig. 5A), suggesting the reduced reactivity to whisker stimulation is not totally due to confounding motor issues. Taken together, our results indicate that *Shank3b*$^{-/-}$ mice display reduced evasive responses to active whisker stimulation, suggesting that *Shank3b*$^{-/-}$ mice are less prone to engage in proactive behaviors in response to novel, invasive tactile stimuli.

Recent studies showed that repetitive whisker stimulation during the WN test results in the altered expression of the activity marker c-Fos in several brain areas of ASD mouse models (Chelini et al. 2019; Pizzo et al. 2020). Whisker stimulation during WN resulted in c-*fos* mRNA downregulation in *Shank3b*$^{-/-}$ S1 and hippocampus (Fig. 3), but not other brain areas (Fig. 4). Accordingly, whisker stimulation under anesthesia selectively downregulated c-*fos* mRNA in the same regions of *Shank3b*$^{-/-}$ mice (Figs 4 and 5). Recent findings showed that *Shank3b*$^{-/-}$ mice exhibit increased sensitivity to whisker stimulation in a vibrissa motion detection task (Chen et al. 2020). Specifically, *Shank3b*$^{-/-}$ mutants showed increased sensitivity to weak but not strong stimuli applied to the whiskers. The authors also showed that this hyper-reactivity to weak tactile stimulation was due to increased excitation/inhibition (E/I) balance resulting from increased firing of excitatory neurons and reduced firing of GABAergic interneurons in S1 (Chen et al. 2020). Accordingly, a reduced expression of the GABAergic marker parvalbumin was detected in *Shank3b*$^{-/-}$ brains (Filice et al. 2016; Orefice et al. 2019). Contrary to Chen et al. (2020), we show that *Shank3b*$^{-/-}$ mice are hypo-reactive to repetitive whisker stimulation (Fig. 2). The different experimental protocols

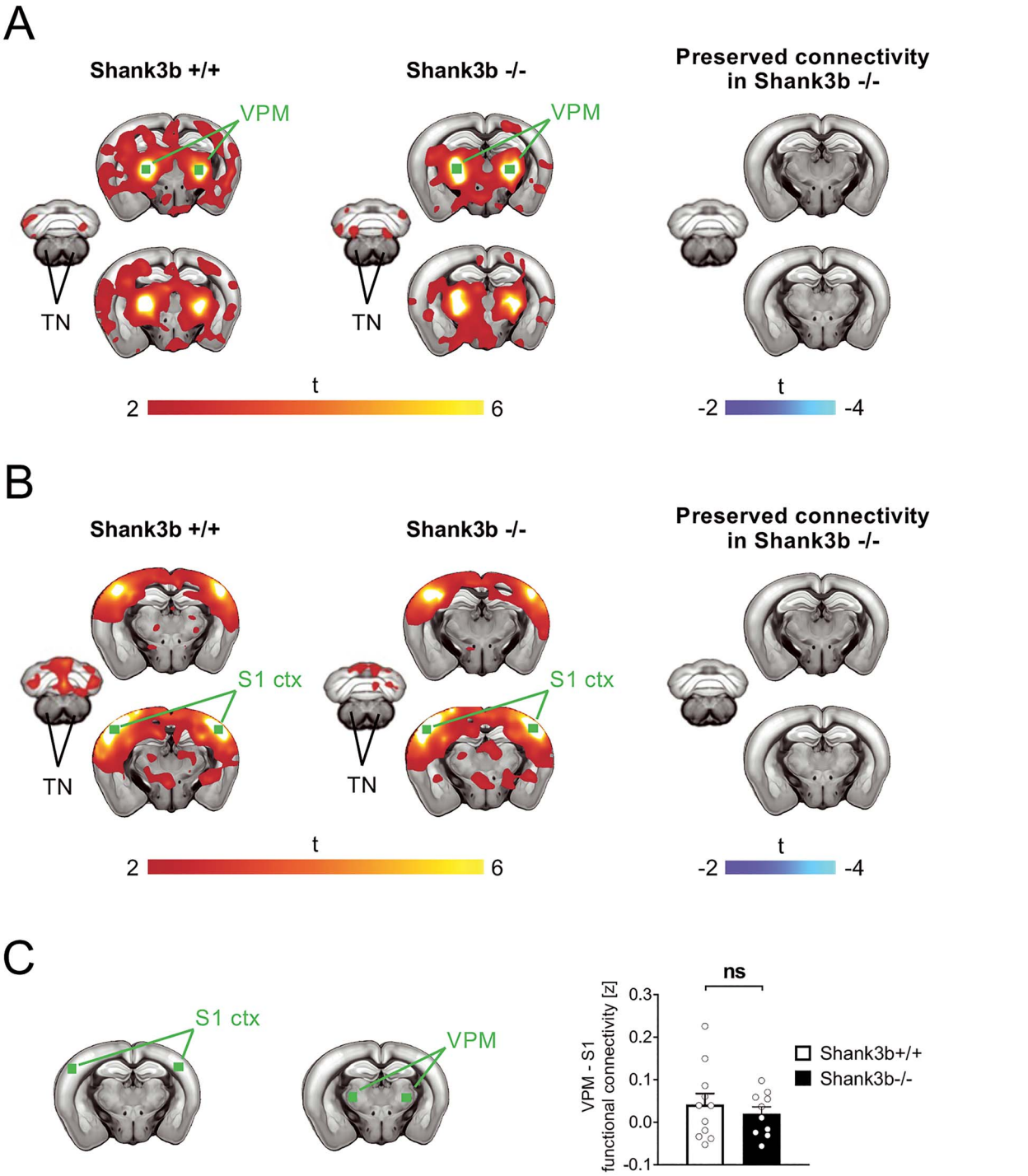

Fig. 6. Preserved functional connectivity between VPM, S1 and TN in *Shank3b*$^{-/-}$ mice. (A) Seed-based connectivity maps of the VPM in *Shank3b*$^{+/+}$ and *Shank3b*$^{-/-}$ mice. Red-yellow represents brain regions showing significant rsfMRI functional connectivity with the VPM in *Shank3b*$^{+/+}$ (left) and *Shank3b*$^{-/-}$ mice (middle). Seed region is depicted in green. Intergroup genotype-dependent comparisons show unimpaired connectivity of the VPM in *Shank3b*$^{-/-}$ mice (right). (B) Seed-based connectivity maps of S1 in *Shank3b*$^{+/+}$ and *Shank3b*$^{-/-}$ mice. Red-yellow represents brain regions showing significant rsfMRI functional connectivity S1 in *Shank3b*$^{+/+}$ (left) and *Shank3b*$^{-/-}$ mice (middle). Seed region is depicted in green. Intergroup genotype-dependent comparisons show preserved functional connectivity of S1 in *Shank3b*$^{-/-}$ mice (right). (C) Region-based quantifications confirmed that functional connectivity between VPM and S1 was unimpaired in *Shank3b*$^{-/-}$ mice, as quantified in reference volumes of interest (green) (unpaired t-test, t = 0.68, $P = 0.50$, n = 11 *Shank3b*$^{+/+}$ and n = 10 *Shank3b*$^{-/-}$ mice; each dot represents one animal). Error bars represent SEM.

used in the two studies (Chen et al. 2020: psychometric, imaging, and electrophysiological measurements following weak whisker stimulation in head-restrained mice; this study: behavioral phenotyping and c-*fos* mRNA expression analysis following repetitive whisker stimulation in freely moving animals) do not allow us to directly compare the obtained results. We also show that, in *Shank3b*$^{-/-}$ mice, whisker-dependent hypo-reactivity is accompanied by the lack of c-*fos* mRNA induction in S1 and hippocampus (Figs 3, 4, and Supplementary Fig. 8), indicating a possible reduction of E/I balance. Further studies are needed to better characterize the neuronal subtypes showing altered c-*fos* mRNA regulation in *Shank3b*$^{-/-}$ mice. The absence of c-*fos* mRNA upregulation observed in *Shank3b*$^{-/-}$ S1 and hippocampus following repetitive whisker stimulation is consistent with synaptic impairment previously shown in *Shank3* mutants (Bozdagi et al. 2010; Yang et al. 2012), and might reflect a diminished neuronal response to repetitive whisker stimulation.

The hippocampus receives inputs from the somatosensory cortex (Lavenex and Amaral 2000), and several studies indicate that many inputs control hippocampal neurons' responses. CA1 pyramidal cells receive information from the whiskers via the somatosensory thalamus (VPM) and entorhinal cortex (Pereira et al. 2007). Somatosensory stimulation increases DG granule cell firing, while predominantly inhibitory responses occur in CA1 (Bellistri et al. 2013). Hippocampal neurons use afferent somatosensory information to dynamically update spatial maps (Pereira et al. 2007). Accordingly, blockade of tactile transmission by applying lidocaine on the whisker pad decreased the firing rate of hippocampal place cells, resulting in expanding their place fields in the rat (Gener et al. 2013). Synchronized activity between S1 and hippocampus is crucial for the formation of cognitive maps. In the rat, coherence between S1 firing and hippocampal activity increases when the animal collects sensory information through whiskers, and such coherence enhances the integration of somatosensory information in the hippocampus (Grion et al. 2016). In mice, tactile experience enrichment induces c-Fos expression in the hippocampus and improves memory by modulating the activity of DG granule cells that receive sensory information from S1 via the entorhinal cortex (Wang et al. 2020). Chemogenetic activation of DG neurons receiving tactile stimuli results in memory enhancement, while inactivation of DG or S1-innervated entorhinal neurons has opposite effects (Wang et al. 2020). Thus, tactile experience modifies cognitive maps by modulating the activity of the S1 to hippocampus pathway, confirming the importance of this circuit in somatosensory information processing. Within this framework, the observed rsfMRI hypo-connectivity between the dorsal hippocampus and S1 might represent a network substrate for the reduced activation of these areas (Figs 3 and 5) and restricted behavioral responses (Fig. 2) following repetitive whisker stimulation in *Shank3b*$^{-/-}$ mice. This conclusion is strengthened by the observation that *Shank3b*$^{-/-}$ mice show a preserved connectivity between S1 and thalamic/brainstem somatosensory areas (Fig. 6).

Aberrant responses to whisker stimulation are frequently detected in mice harboring ASD-relevant mutations (Balasco et al. 2020), suggesting that whisker-dependent behaviors are a good proxy for tactile defensiveness that is often observed in ASD (Mikkelsen et al. 2018) and specifically in PMS (Tavassoli et al. 2021). Our findings suggest that impaired crosstalk between hippocampus and S1 might underlie hypo-reactivity to whisker-dependent cues in *Shank3b*$^{-/-}$ mice. Further studies are needed to extend these findings to ASD.

Supplementary material

Supplementary material can be found at *Cerebral Cortex* online.

Author contributions

LB designed and performed behavioral and in situ hybridization experiments, analyzed data, and wrote the manuscript; MP performed rsfMRI experiments, analyzed data, and drafted the paper; LP, AGCC, ES, and LM performed behavioral experiments; GC analyzed data and drafted the paper; AGa provided technical assistance for rsfMRI experiments; GI performed whisker stimulation experiments in head-fixed animals, drafted the paper, and provided funding; GP performed behavioral experiments and edited the manuscript; AGo designed rsfMRI experiments, analyzed data, provided funding, and edited the manuscript; YB performed in situ hybridization experiments, analyzed data, supervised the whole study, provided funding, and wrote the manuscript.

Funding

This work was supported by the Strategic Project TRAIN—Trentino Autism Initiative (https://projects.unitn.it/train/index.html) from the University of Trento (grant 2018–2021 to YB). LB is a recipient of a PhD fellowship from the University of Trento and Fondazione CARITRO (Trento, Italy). LP is supported by a postdoctoral fellowship from the Umberto Veronesi Foundation (Milan, Italy). GC was supported by a postdoctoral fellowship from CIMeC/University of Trento. GP is supported by the Brain and Behavior Research Foundation (NARSAD Young Investigator Grant; ID: 26617) and the University of Trento (Starting Grant for Young Researchers). GI was funded by the Armenise Harvard Foundation (Career Development Award). AGo was funded by the Simons Foundation (SFARI 400101), Brain and Behavior Foundation (NARSAD—National Alliance for Research on Schizophrenia and Depression), the European Research Council (ERC-DISCONN, GA802371), the NIH (1R21MH116473-01A1) and the Telethon Foundation (GGP19177).

Notes

YB dedicates this study to the memory of Paolo Sassone-Corsi, a great scientist and a dear friend, who unexpectedly left us on 22 July 2020. The c-*fos* cDNA used to prepare riboprobes for in situ hybridization experiments was a kind gift of Paolo's laboratory in 1997. The authors thank the technical and administrative staff of CIMeC, CIBIO, and IIT for assistance. *Conflict of Interest*: None declared.

References

Ahl AS. 1986. The role of vibrissae in behavior: a status review. *Vet Res Commun*. 10:245–268.

American Psychiatric Association DSMTF. 2013. *Diagnostic and statistical manual of mental disorders: DSM-5*. Arlington, VA: American Psychiatric Association.

Angelakos CC, Tudor JC, Ferri SL, Jongens TA, Abel T. 2019. Home-cage hypoactivity in mouse genetic models of autism spectrum disorder. *Neurobiol Learn Mem*. 165:107000.

Balasco L, Chelini G, Bozzi Y, Provenzano G. 2019. Whisker nuisance test: a valuable tool to assess tactile hypersensitivity in mice. *Bio Protocol*. 9:e3331.

Balasco L, Provenzano G, Bozzi Y. 2020. Sensory abnormalities in autism spectrum disorders: a focus on the tactile domain, from genetic mouse models to the clinic. *Front Psych*. 10:1016.

Bellistri E, Aguilar J, Brotons-Mas JR, Foffani G, de la Prida LM. 2013. Basic properties of somatosensory-evoked responses in the dorsal hippocampus of the rat. *J Physiol*. 591:2667–2686.

Bertero A, Liska A, Pagani M, Parolisi R, Masferrer ME, Gritti M, Pedrazzoli M, Galbusera A, Sarica A, Cerasa A, et al. 2018. Autism-associated 16p11.2 microdeletion impairs prefrontal functional connectivity in mouse and human. *Brain*. 141:2055–2065.

Bozdagi O, Sakurai T, Papapetrou D, Wang X, Dickstein DL, Takahashi N, Kajiwara Y, Yang M, Katz AM, Scattoni ML, et al. 2010. Haploinsufficiency of the autism-associated Shank3 gene leads to deficits in synaptic function, social interaction, and social communication. *Mol Autism*. 1:15.

Bozzi Y, Vallone D, Borrelli E. 2000. Neuroprotective role of dopamine against hippocampal cell death. *J Neurosci*. 20:8643–8649.

Brecht M. 2007. Barrel cortex and whisker-mediated behaviors. *Curr Op Neurobiol*. 17:408–416.

Chelini G, Zerbi V, Cimino L, Grigoli A, Markicevic M, Libera F, Robbiati S, Gadler M, Bronzoni S, Miorelli S, et al. 2019. Aberrant somatosensory processing and connectivity in mice lacking Engrailed-2. *The J Neurosci*. 39:1525–1538.

Chen Q, Deister CA, Gao X, Guo B, Lynn-Jones T, Chen N, Wells MF, Liu R, Goard MJ, Dimidschstein J, et al. 2020. Dysfunction of cortical GABAergic neurons leads to sensory hyper-reactivity in a Shank3 mouse model of ASD. *Nat Neurosci*. 23:520–532.

Diamond ME, Arabzadeh E. 2013. Whisker sensory system - from receptor to decision. *Prog Neurobiol*. 103:28–40.

Diamond ME, von Heimendahl M, Knutsen PM, Kleinfeld D, Ahissar E. 2008. 'Where' and 'what' in the whisker sensorimotor system. *Nat Rev Neurosci*. 9:601–612.

Domínguez-Iturza N, Lo AC, Shah D, Armendáriz M, Vannelli A, Mercaldo V, Trusel M, Li KW, Gastaldo D, Santos AR, et al. 2019. The autism- and schizophrenia-associated protein CYFIP1 regulates bilateral brain connectivity and behaviour. *Nat Commun*. 10:3454. https://doi.org/10.1038/s41467-019-11203-y.

Filice F, Vörckel KJ, Sungur AÖ, Wöhr M, Schwaller B. 2016. Reduction in parvalbumin expression not loss of the parvalbumin-expressing GABA interneuron subpopulation in genetic parvalbumin and shank mouse models of autism. *Mol Brain*. 9:10.

Filipkowski RK, Rydz M, Berdel B, Morys J, Kaczmarek L. 2000. Tactile experience induces c-fos expression in rat barrel cortex. *Learn Mem*. 7:116–122.

Foss-Feig JH, Heacock JL, Cascio CJ. 2012. Tactile responsiveness patterns and their association with core features in autism spectrum disorders. *Res Autism Spectr Disord*. 6:337–344.

Gener T, Perez-Mendez L, Sanchez-Vives MV. 2013. Tactile modulation of hippocampal place fields. *Hippocampus*. 23:1453–1462.

Grion N, Akrami A, Zuo Y, Stella F, Diamond ME. 2016. Coherence between rat sensorimotor system and hippocampus is enhanced during tactile discrimination. *PLoS Biol*. 14:e1002384.

Haberl MG, Zerbi V, Veltien A, Ginger M, Heerschap A, Frick A. 2015. Structural-functional connectivity deficits of neocortical circuits in the Fmr1−/y mouse model of autism. *Sci Adv*. 1:e1500775.

He CX, Cantu DA, Mantri SS, Zeiger WA, Goel A, Portera-Cailliau C. 2017. Tactile defensiveness and impaired adaptation of neuronal activity in the Fmr1 knock-out mouse model of autism. *J Neurosci*. 37:6475–6487.

Jaramillo TC, Speed HE, Xuan Z, Reimers JM, Escamilla CO, Weaver TP, Liu S, Filonova I, Powell CM. 2017. Novel Shank3 mutant exhibits behaviors with face validity for autism and altered striatal and hippocampal function. *Autism Res*. 10:42–65.

Jiang YH, Ehlers MD. 2013. Modeling autism by SHANK gene mutations in mice. *Neuron*. 78:8–27.

Lavenex P, Amaral DG. 2000. Hippocampal-neocortical interaction: a hierarchy of associativity. *Hippocampus*. 10:420–430.

Leblond CS, Nava C, Polge A, Gauthier J, Huguet G, Lumbroso S, Giuliano F, Stordeur C, Depienne C, Mouzat K, et al. 2014. Meta-analysis of SHANK mutations in autism spectrum disorders: a gradient of severity in cognitive impairments. *PLoS Genet*. 10:e1004580.

Liska A, Bertero A, Gomolka R, Sabbioni M, Galbusera A, Barsotti N, Panzeri S, Scattoni ML, Pasqualetti M, Gozzi A. 2018. Homozygous loss of autism-risk gene CNTNAP2 results in reduced local and long-range prefrontal functional connectivity. *Cereb Cortex*. 28:1141–1153.

Mammen MA, Moore GA, Scaramella LV, Reiss D, Ganiban JM, Shaw DS, Leve LD, Neiderhiser JM. 2015. Infant avoidance during a tactile task predicts autism spectrum behaviors in toddlerhood. *Infant Ment Health J*. 36:575–587.

Michetti C, Caruso A, Pagani M, Sabbioni M, Medrihan L, David G, Galbusera A, Morini M, Gozzi A, Benfenati F, et al. 2017. The knockout of synapsin II in mice impairs social behavior and functional connectivity generating an ASD-like phenotype. *Cereb Cortex*. 27:5014–5023.

Mikkelsen M, Wodka EL, Mostofsky SH, Puts NAJ. 2018. Autism spectrum disorder in the scope of tactile processing. *Dev Cogn Neurosci*. 29:140–150.

Monteiro P, Feng G. 2017. SHANK proteins: roles at the synapse and in autism spectrum disorder. *Nat Rev Neurosci*. 18:147–157.

Naisbitt S, Kim E, Tu JC, Xiao B, Sala C, Valtschanoff J, Weinberg RJ, Worley PF, Sheng M. 1999. Shank, a novel family of postsynaptic density proteins that binds to the NMDA receptor/PSD-95/GKAP complex and cortactin. *Neuron*. 23:569–582.

Orefice LL. 2020. Peripheral somatosensory neuron dysfunction: emerging roles in autism spectrum disorders. *Neuroscience*. 445:120–129.

Orefice LL, Mosko JR, Morency DT, Wells MF, Tasnim A, Mozeika SM, Ye M, Chirila AM, Emanuel AJ, Rankin G, et al. 2019.

Targeting peripheral somatosensory neurons to improve tactile-related phenotypes in ASD models. *Cell*. 178:867–886.

Orefice LL, Zimmerman AL, Chirila AM, Sleboda SJ, Head JP, Ginty DD. 2016. Peripheral mechanosensory neuron dysfunction underlies tactile and behavioral deficits in mouse models of ASDs. *Cell*. 166:299–313.

Pagani M, Bertero A, Liska A, Galbusera A, Sabbioni M, Barsotti N, Colenbier N, Marinazzo D, Scattoni ML, Pasqualetti M, et al. 2019. Deletion of autism risk gene Shank3 disrupts prefrontal connectivity. *J Neurosci*. 39:5299.

Pagani M, Bertero A, Trakoshis S, Ulysse L, Locarno A, Miseviciute I, De Felice A, Canella C, Supekar K, Galbusera A, et al. 2021. mTOR-related synaptic pathology causes autism spectrum disorder-associated functional hyperconnectivity. *Nat Commun*. 12:6084.

Peça J, Feliciano C, Ting JT, Wang W, Wells MF, Venkatraman TN, Lascola CD, Fu Z, Feng G. 2011. Shank3 mutant mice display autistic-like behaviours and striatal dysfunction. *Nature*. 472: 437–442.

Pereira A, Ribeiro S, Wiest M, Moore LC, Pantoja J, Lin S-C, Nicolelis MAL. 2007. Processing of tactile information by the hippocampus. *Proc Natl Acad Sci U S A*. 104:18286–18291.

Petersen CC. 2007. The functional organization of the barrel cortex. *Neuron*. 56:339–355.

Phelan K, McDermid HE. 2012. The 22q13.3 deletion syndrome (Phelan-McDermid syndrome). *Mol Syndromol*. 2:186–201.

Philippe A, Boddaert N, Vaivre-Douret L, Robel L, Danon-Boileau L, Malan V, de Blois M-C, Heron D, Colleaux L, Golse B, et al. 2008. Neurobehavioral profile and brain imaging study of the 22q13.3 deletion syndrome in childhood. *Pediatrics*. 122:e376.

Pizzo R, Lamarca A, Sassoè-Pognetto M, Giustetto M. 2020. Structural bases of atypical whisker responses in a mouse model of CDKL5 deficiency disorder. *Neuroscience*. 445:130–143.

Provenzano G, Pangrazzi L, Poli A, Pernigo M, Sgadò P, Genovesi S, Zunino G, Berardi N, Casarosa S, Bozzi Y. 2014. Hippocampal dysregulation of neurofibromin-dependent pathways is associated with impaired spatial learning in engrailed 2 knock-out mice. *J Neurosci*. 34:13281–13288.

Robertson CE, Baron-Cohen S. 2017. Sensory perception in autism. *Nat Rev Neurosci*. 18:671–684.

Schmucker C, Seeliger M, Humphries P, Biel M, Schaeffel F. 2005. Grating acuity at different luminances in wild-type mice and in mice lacking rod or cone function. *Invest Ophthalmol Vis Sci*. 46: 398–407.

Sforazzini F, Bertero A, Dodero L, David G, Galbusera A, Scattoni ML, Pasqualetti M, Gozzi A. 2016. Altered functional connectivity networks in acallosal and socially impaired BTBR mice. *Brain Struct Funct*. 221:941–954.

Tavassoli T, Layton C, Levy T, Rowe M, George-Jones J, Zweifach J, Lurie S, Buxbaum JD, Kolevzon A, Siper PM. 2021. Sensory reactivity phenotype in Phelan-McDermid syndrome is distinct from idiopathic ASD. *Genes (Basel)*. 12:977. https://doi.org/10.3390/genes12070977.

Tripathi PP, Sgadò P, Scali M, Viaggi C, Casarosa S, Simon HH, Vaglini F, Corsini GU, Bozzi Y. 2009. Increased susceptibility to kainic acid-induced seizures in Engrailed-2 knockout mice. *Neuroscience*. 159:842–849.

Unichenko P, Yang JW, Kirischuk S, Kolbaev S, Kilb W, Hammer M, Krueger-Burg D, Brose N, Luhmann HJ. 2018. Autism related neuroligin-4 knockout impairs intracortical processing but not sensory inputs in mouse barrel cortex. *Cereb Cortex*. 28:2873–2886.

Wang C, Liu H, Li K, Wu ZZ, Wu C, Yu JY, Gong Q, Fang P, Wang XX, Duan SM, et al. 2020. Tactile modulation of memory and anxiety requires dentate granule cells along the dorsoventral axis. *Nat Commun*. 11:6045.

Wu HP, Ioffe JC, Iverson MM, Boon JM, Dyck RH. 2013. Novel, whisker-dependent texture discrimination task for mice. *Behav Brain Res*. 237:238–242.

Yang M, Bozdagi O, Scattoni ML, Wöhr M, Roullet FI, Katz AM, Abrams DN, Kalikhman D, Simon H, Woldeyohannes L, et al. 2012. Reduced excitatory neurotransmission and mild autism-relevant phenotypes in adolescent Shank3 null mutant mice. *J Neurosci*. 32: 6525–6541.